The Spine Journal 19 (2019) 744–754

Basic Science

Mechanical performance of traditional distraction-based dual growing rod constructs

Genevieve Hill, BS[a,b,*], Srinidhi Nagaraja, PhD[a], Austin Bridges[a], Ardalan Seyed Vosoughi, MS[c], Vijay K. Goel, PhD[c], Maureen L. Dreher, PhD[a]

[a] *U.S. Food and Drug Administration, 10903 New Hampshire Ave, Silver Spring, MD, 20993, USA*
[b] *University of Maryland, College Park, College Park, MD 20742*
[c] *Engineering Center for Orthopaedic Research Excellence, Department of Bioengineering and Orthopaedic Surgery, Colleges of Engineering and Medicine, University of Toledo, Toledo, OH, 43606, USA*
Received 17 May 2018; revised 31 August 2018; accepted 5 September 2018

Abstract

BACKGROUND: Growing rod constructs are an important contribution in the treatment of children with early onset scoliosis even though these devices experience high rates of rod fracture. The mechanical performance of traditional, distraction-based dual growing rod constructs is not well understood, and mechanical models for predicting device performance are limited.

PURPOSE: Two mechanical models were developed and used to determine the mechanical performance of various growing rod configurations by increasing construct complexity.

STUDY DESIGN/SETTING: Mechanical bench testing and finite element (FE) analysis.

METHODS: Static and dynamic compression bending tests were based on an ASTM F1717 method modified to accommodate dual growing rod constructs. Six construct configurations were tested, mechanical properties were recorded, and statistical analyses were performed to determine significant differences between groups: (1) no connectors (rods only), (2) side-by-side connectors, (3) side-by-side connectors plus 4 crosslinks, (4) (40-mm long tandem connectors, (5) 80-mm long tandem connectors, and (6) 80-mm long tandem connectors plus 4 crosslinks. FE analysis was used to predict the stress distribution within the constructs.

RESULTS: The static results indicated greater stiffness, yield load, and peak load as the axial connector length increased (side-by-side to 40 mm tandem to 80 mm tandem). The dynamic results showed similar cycles to failure for side-by-side and tandem connector (40 and 80 mm) construct configurations without crosslinks. Crosslinks shifted the location of rod fracture observed experimentally and significantly reduced the fatigue life of the construct. The flexibility of the construct decreased significantly as the axial connector length increased. FE predictions were highly consistent with the experimentally measured values and provided information on stress distribution within the rod for comparison to experimental fracture locations.

CONCLUSIONS: This is the first study to evaluate mechanical performance of various configurations of pediatric growing rod constructs using preclinical models. The current study is consistent with a previous retrieval study in that rigid constructs lacking flexibility (ie, higher stiffness and lower displacement), such as those with 80-mm tandem connectors and multiple crosslinks, demonstrated decreased mechanical performance as shown through both experimental and computational models. Additionally, the experimental and computational findings suggest that surgeons should strategically consider the number of interconnecting components and subsequent stress concentrations along the posterior side of the rod. For example, changing the placement of crosslinks to low stress regions of the construct or not using crosslinks in the construct are options. Published by Elsevier Inc.

FDA device/drug status: Not applicable.

Author disclosures: ***GH:*** Nothing to disclose. ***SN:*** Nothing to disclose. ***AB:*** Nothing to disclose. ***ASV:*** Nothing to disclose. ***VKG:*** Consulting: DePuy (D, Paid directly to institution/employer); Device or Biologic Distribution Group (Physician-Owned Distributorship): Butterfly, LLC (C), Endosphere, LLC (C), Globus Spine (C); Grants: DePuy (E, Paid directly to institution/employer); Scientific Advisory Board: Turning Point, LLC (Nonfinancial); Stock Ownership: BONE LLC (33%). ***MLD:*** Nothing to disclose.

* Corresponding author. U.S. Food and Drug Administration, 10903 New Hampshire Ave, Silver Spring, MD, 20993, USA.
E-mail address: genevieve.mcrae@fda.hhs.gov (G. Hill).

https://doi.org/10.1016/j.spinee.2018.09.006
1529-9430/Published by Elsevier Inc.

Keywords: Computational or finite element analysis model; Early onset scoliosis; Growing rod; Mechanical or bench testing; Pediatric; Spinal instrumentation.

Introduction

Traditional, distraction-based growing rod constructs used in children with early onset scoliosis have unique features compared with spinal instrumentation used in adult deformity or fusion applications. One unique feature of these constructs is the ability of the surgeon to use a variety of configurations to achieve rod lengthening via axial connectors and encourage growth of a deformed spine and thorax [1]. The axial connectors join the longitudinal rods either in a parallel orientation (known as a side-by-side or wedding band connector) or in series where the rods are placed into each end of the connector (known as a tandem connector). Crosslinks, also known as cross connectors, are optional components used in the growing rod constructs to help increase the torsional rigidity by connecting the parallel longitudinal rods [2–7]. The surgeon's selection of the axial connector type or length as well as the quantity of crosslinks is primarily based on surgeon preference and patient anatomy, resulting in numerous possibilities of construct configurations. Given that growing rod treatment is associated with high complication rates [8–15], it is important to understand the biomechanical differences between various construct configurations and the subsequent impact on device failure.

The relationship between rod fracture and construct configuration in traditional, distraction-based growing rod constructs is not well understood. As identified from a registry analysis, Yang et al. concluded that rod fracture was associated with longer tandem connectors, but the connector length was not reported [13]. Yamaguchi et al. hypothesized that less rigid constructs allow for more "mechanical slop" (or flexibility) and, therefore, were associated with less rod breakage, but mechanical testing was not done to support this hypothesis [16]. The connector-rod interface was explored by Lee et al., but was limited to loosening only and did not include an evaluation of rod fracture [17]. Mahar et al. focused their investigation on biomechanical differences between anchor configurations and, therefore, did not evaluate the growing rod construct as a whole or correlate their findings with rod fracture [18]. In a previous retrieval study, it was reported that the combined use of tandem connectors and multiple crosslinks (2 or more) was associated with fracture of growing rod constructs whereas intact constructs were typically configured without crosslinks and with side-by-side or tandem connectors [19]. These prior studies indicated that certain configurations may provide better mechanical integrity over others, but they were not able to identify which construct components have the greatest impact on mechanical performance. Therefore, a systematic investigation of construct complexity is necessary to determine the mechanical performance of various construct configurations. This need further necessitates the development of a nonclinical, mechanical model that can evaluate the complete construct and is representative of relevant spine biomechanical loading associated with fracture. Such a model is lacking in the literature. A nonclinical model is critical to help us understand the contribution of each implant component on the performance of the entire construct, which may help refine surgical techniques. In addition, the model can serve as a tool for evaluating improvements in implant design.

The objective of the current study was to determine the mechanical performance of various configurations of traditional, distraction-based dual growing rod constructs with increasing complexity. To achieve this objective, both experimental and computational models were developed. The mechanical bench model was used to evaluate the mechanical performance of constructs with increasing complexity. The computational model served to complement the experimental model by predicting the stress distribution within the construct and identifying regions of high stress likely to result in fracture.

Methods

Growing rod construct configurations

The mechanical bench model was based upon compression-bending static and fatigue loading of spinal implants described in ASTM F1717—*Standard Test Methods for Spinal Implant Constructs in a Vertebrectomy Model* [20], but the specimen setup was modified to accommodate growing rod devices. The specimen setup consisted of growing rod components configured into ultrahigh molecular weight polyethylene (UHMWPE) test blocks and loaded in compression-bending such that the posterior side of the rod was in tension. The compression-bending loading mode were selected based upon the results of a prior retrieval study which identified that rod fracture in vivo initiates from compression-bending on the posterior side of the rod due to flexion motion [19]. All device configurations included eight Ø4.5 mm polyaxial pedicle screws inserted fully into the test blocks (deviation from the standard, which outlines four screws that are not fully inserted), set screws, and bilateral Ø4.5 mm rods. Construct complexity was investigated by measuring the mechanical performance of six different configurations based on the types and lengths of connectors used (Table 1): (1) no connectors (rods only), (2) side-by-side connectors, (3) side-by-side connectors plus 4 crosslinks, (4) 40-mm long tandem connectors, (5) 80-mm long tandem connectors, and (6) 80-mm long tandem connectors plus 4 crosslinks.

Table 1
Photographs of the six construct configurations. The top row displays the constructs without crosslinks: No connectors—rods only, side-by-side connectors, 40-mm tandem connectors, and 80-mm tandem connectors. The bottom row displays the constructs with crosslinks: Side-by-side connectors plus 4 crosslinks and 80-mm tandem connectors plus 4 crosslinks. All construct configurations have an active length of 200 mm and the axial connectors are placed in the center of the construct (note: constructs with side-by-side connectors have offset pedicle screws in the superior test blocks). Fixtures include steel U-frames with pins attached to UHMWPE test blocks with the load cell on the bottom

	No connectors—rods only	Side-by-side connectors	40-mm Tandem connectors	80-mm Tandem connectors
Construct configurations without crosslinks		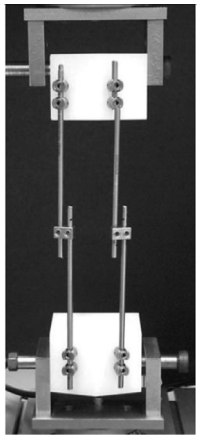		
Construct configurations with crosslinks	n/a		n/a	

The axial connectors were placed in the center of the construct, and the construct active length, which was measured as the distance between the interior pedicle screws, was consistent between all test groups at 200 mm (deviation from the standard that lists a 76-mm active length for thoracolumbar constructs) based upon average rod lengths reported in a prior retrieval study [19]. The pedicle screws were located in the same location of the test blocks for all configurations, except the side-by-side connector constructs, which included offset screws in the superior test block in order to keep the rods parallel to the direction of applied load (deviation from the standard where all screws are centered in the test block). The construct configurations with crosslinks included two crosslinks at the proximal end and two crosslinks at the distal end for a total of four crosslinks in the high stress regions. The set screws were torqued to 60 in-lbs using a torque-limiting wrench. All components were made from Titanium alloy (Ti6Al4V) per ASTM F136 [21].

Static testing

Static compression bending tests were performed for each construct configuration using a calibrated mechanical load frame (Instron E3000, Norwood, MA) and calibrated 1 kN load cell (Instron Dynacell, Norwood, MA). A displacement-controlled rate of 25 mm/min compression was applied until

a total displacement of 50 mm was reached. Six samples for each configuration were tested in ambient conditions for a total of 36 static compression bending samples. Load and displacement data were captured throughout the test and used to calculate stiffness, yield load, and peak load according to ASTM F1717 (MATLAB, MathWorks, Natick, MA) [20].

Dynamic testing

Dynamic compression bending tests were also performed for each construct configuration using the same mechanical load frame and load cell. A load-controlled test was performed at 4 Hz between 150 N and 15 N compressive loads (R = 0.1) per a sinusoidal waveform until rod fracture occurred. Eight samples for each configuration were tested in ambient conditions for a total of 48 dynamic compression bending samples. Cycles to failure were based on change to either the maximum and/or minimum displacement or the peak/valley load readings. Displacements were retrieved from the dataset at the following cycles to determine how flexibility of the construct changed over time: 5000 cycles after start of the test, 50,000 cycles after start of the test, and 1000 cycles before failure. At each of these time points, the change in displacement was calculated by subtracting the displacements reached at the maximum and minimum loads. Fracture location within the construct was recorded and the fracture initiation site was determined through evaluation using optical microscopy (Hirox-USA KH-7700, Hackensack, NJ) and scanning electron microscopy (SEM, JEOL USA JSM-6390LV) as described previously [19].

Computational modeling

Finite element (FE) analysis of the compression bending test was performed on all six construct configurations. The components of each construct were precisely designed and assembled in accordance with their experimental counterparts in SolidWorks (Dassault Systèmes SolidWorks Corporation, Waltham, MA) and imported into ABAQUS/Standard v6-14 (Dassault Systèmes, Simulia, Waltham, MA) for stress analysis. The rods were meshed using eight-node hexahedral elements (C3D8) with an element size of 0.5 mm, whereas all other components were discretized with four-node tetrahedral elements (C3D4) that had variable element sizes depending on the function and size of the component. The mesh density for each construct configuration was determined from a preliminary mesh convergence study, which identified the converged mesh based on a 3% change or less in construct stiffness. A tie constraint was used to bond the screw-block, screw-set screw, rod-tulip, rod-tandem, and rod-crosslink interfaces. In each construct, the blocks were modeled as UHMWPE (modulus of elasticity (E) = 690 MPa, Poisson's ratio (ν) = 0.46) whereas all other components (ie, rods, pedicle and set screws, axial connectors, and crosslinks) were modeled as elasto-plastic Ti6Al4V (E = 105000 MPa, yield stress = 600 MPa, $\nu = 0.3$) with isotropic hardening based on stress–strain data obtained from the titanium vendor.

In order to simulate compression bending in each construct, 50 mm displacement was applied at a reference point located in the center of the pin hole of the superior block. The reference point was kinematically coupled to the inner surface of the pin hole. The distal test block was constrained such that it was only allowed to rotate about the flexion-extension axis (Supplementary Fig. 1). For each construct, the load–displacement curves as predicted by the FE analysis were compared with those measured experimentally. The percent difference in FE predicted force as compared with the force measured experimentally for each displacement iteration was calculated and averaged in order to assess the accuracy of model predictions. The FE analysis was further used to predict the stress distribution within construct components and identify critical stress locations for comparison with experimentally observed fractures. Stress values within important construct regions were used to calculate a fatigue safety factor (FSF) using a Goodman analysis. In this analysis, the maximum principal stress at the maximum and minimum applied loads (ie, 150 N and 15 N) was used to calculate the alternating and mean stress. The mean and alternating stress were then compared against the Goodman line, which connects the endurance limit (566 MPa) for Ti6Al4V to its ultimate stress (950 MPa) in order to calculate the FSF.

Statistical analysis

The static test results were normalized to the mean results of the baseline construct configuration, that is no connectors—rods only. An analysis of variance was used to assess statistical differences in all mechanical properties between construct configurations at a significance level of $p \leq .05$ (Minitab Statistical Software, State College, PA). If the overall analysis of variance showed significance, pairwise post-hoc comparisons were executed using Fisher's least significant difference method and 95% confidence.

Results

Static testing

All constructs experienced permanent deformation of the rods when loaded statically. A representative load–displacement curve with calculated mechanical parameters is shown in Fig. 1. Table 2 summarizes the normalized mechanical parameters for all construct configurations. When axial connectors were present, the configurations with side-by-side connectors exhibited the lowest stiffness values, yield loads, and peak loads. Additionally, yield and peak loads for these constructs were similar to those from

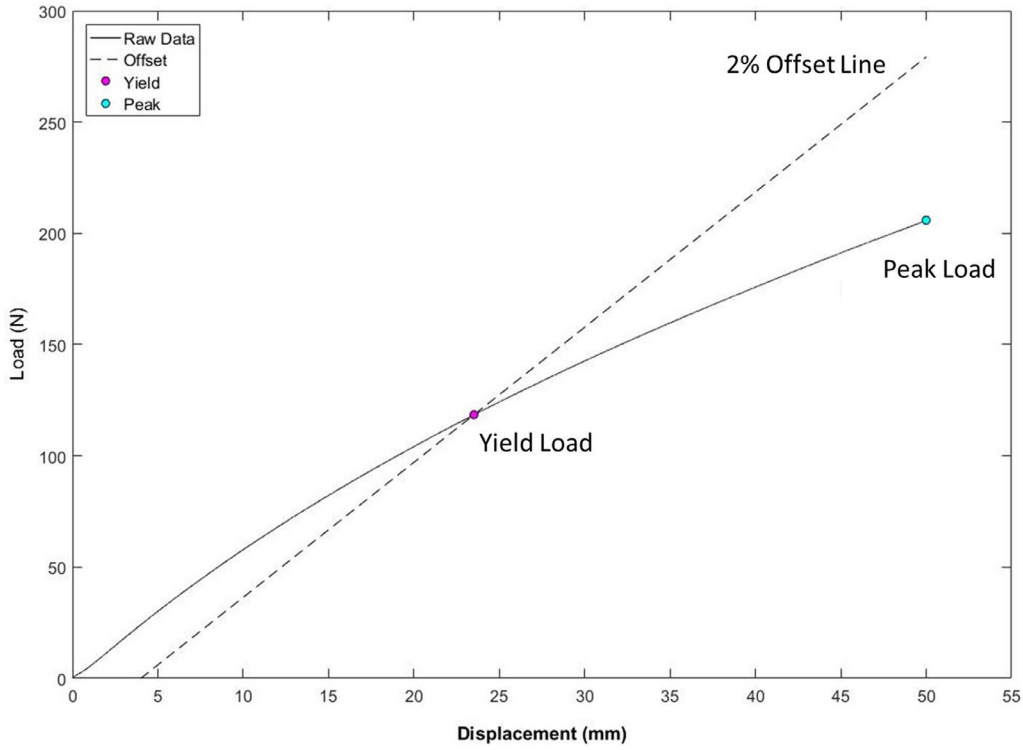

Fig. 1. Sample load–displacement curve software for static compression bending tests. Stiffness was calculated using the 2% offset method in accordance with ASTM F1717. Yield load (pink circle) was the point where the offset (dashed line) intersected the curve (solid line). Peak load (blue circle) was based on the maximum load achieved at 50-mm total displacement. (Color version of figure is available online.).

the no connector (rods only) construct group ($p > .4$). All mechanical parameters (stiffness, yield load, peak load) significantly increased when the axial connector was changed from a side-by-side connector to a tandem connector. For configurations with tandem connectors, the results indicated greater stiffness, yield load, and peak load as the tandem connector length increased from 40 to 80 mm ($p < .001$).

The effect of adding crosslinks to the constructs was variable. The configuration containing an 80-mm tandem connector with crosslinks had a significantly higher stiffness than the 80-mm tandem connector configuration without crosslinks ($p < .001$). However, when a crosslink was included in configurations constructed using the side-by-side connector, the stiffness was significantly lower ($p < .001$). Yield load was not significantly affected by the addition of crosslinks for either the 80-mm tandem or side-by-side connector groups ($p > .1$).

Dynamic testing

All dynamic constructs failed due to rod fracture, with fractures initiating on the posterior side of the rod. The fatigue results are displayed in Fig. 2. The results showed that construct configurations with an axial connector alone (side-by-side, 40 mm tandem, and 80 mm tandem) had similar cycles to failure ($p > .07$). Interestingly, the cycles to failure for the construct configuration without connectors (rods only) was only significantly different than that of the 40-mm tandem connector configuration ($p = .002$). The two construct

Table 2
Results of static compression bending tests. All results have been normalized to the mean results of the baseline construct configuration, that is, no connectors—rods only. The normalized values are presented as a ratio compared with baseline. Stiffness was collected in units of N/mm, and yield and peak loads were collected in units of N. Values in each row that do not share a superscript number, letter, or symbol are significantly different

	Side-by-side connectors		40-mm Tandem connectors	80-mm Tandem connectors	
	Without crosslinks	*With crosslinks*	*Without crosslinks*	*Without crosslinks*	*With crosslinks*
Normalized stiffness					
Mean ± St. deviation	1.033 ± 0.019 [1]	0.957 ± 0.019 [2]	1.169 ± 0.021 [3]	1.518 ± 0.007 [4]	1.611 ± 0.026 [5]
Normalized yield load					
Mean ± St. deviation	0.983 ± 0.025 [A]	0.994 ± 0.021 [A]	1.251 ± 0.0274 [B]	1.639 ± 0.032 [C]	1.671 ± 0.042 [C]
Normalized peak load					
Mean ± St. deviation	0.991 ± 0.011 *	0.951 ± 0.012 [Δ]	1.192 ± 0.007 [#]	1.490 ± 0.011 [Σ]	1.515 ± 0.007 +

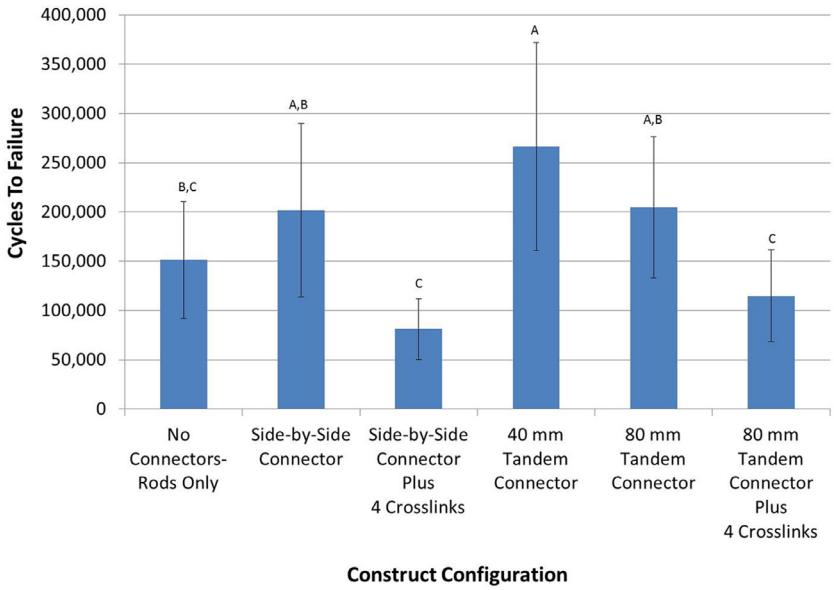

Fig. 2. Fatigue performance for each construct configuration was captured through the number of cycles to failure during dynamic testing (note: error bars represent the standard deviations). All constructs were tested until rod fracture. Groups that do not share a letter are significantly different. Crosslinks significantly decreased the fatigue life of the constructs. Side-by-side and tandem connectors, regardless of length, have similar fatigue lives.

configurations with crosslinks failed significantly earlier than their corresponding counterparts without crosslinks ($p < .015$). All four construct configurations without crosslinks experienced rod fracture adjacent to the pedicle screw whereas both construct configurations with crosslinks experienced rod fracture adjacent to the crosslink (Fig. 3).

The displacements during fatigue cycling varied based on the type and length of axial connector (Fig. 4). All three of the construct configurations with tandem connectors (40 or 80 mm) experienced significantly lower displacements ($p < .001$) during fatigue testing at all time points as compared with groups that lacked a tandem connector (ie, no connectors, side-by-side connectors with or without crosslinks). The two constructs with 80-mm tandem connectors exhibited significantly lower displacements than those present in configurations with 40-mm tandem connectors ($p < .01$) and showed the lowest amount of displacement during fatigue testing overall. In general, the addition of crosslinks to the construct configuration did not alter the fatigue displacement as compared with its counterpart without crosslinks.

Computational modeling

Computational predictions of the compression bending load–displacement curve for all construct configurations

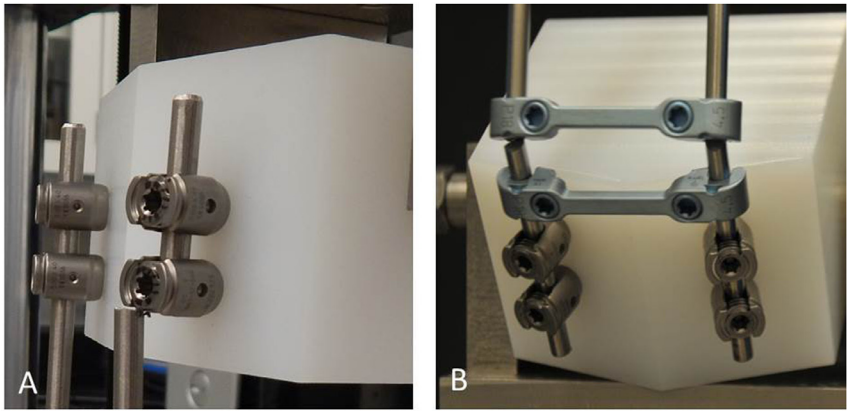

Fig. 3. Examples of rod fracture after fatigue testing. The rods fractured adjacent to the pedicle screw (A) in four construct configurations. The remaining two construct configurations had crosslinks, and the location of rod fractures shifted adjacent to the crosslink (B). In all cases, fractures initiated on the posterior side of the rod adjacent to a stress concentration due to either the pedicle screws or crosslinks.

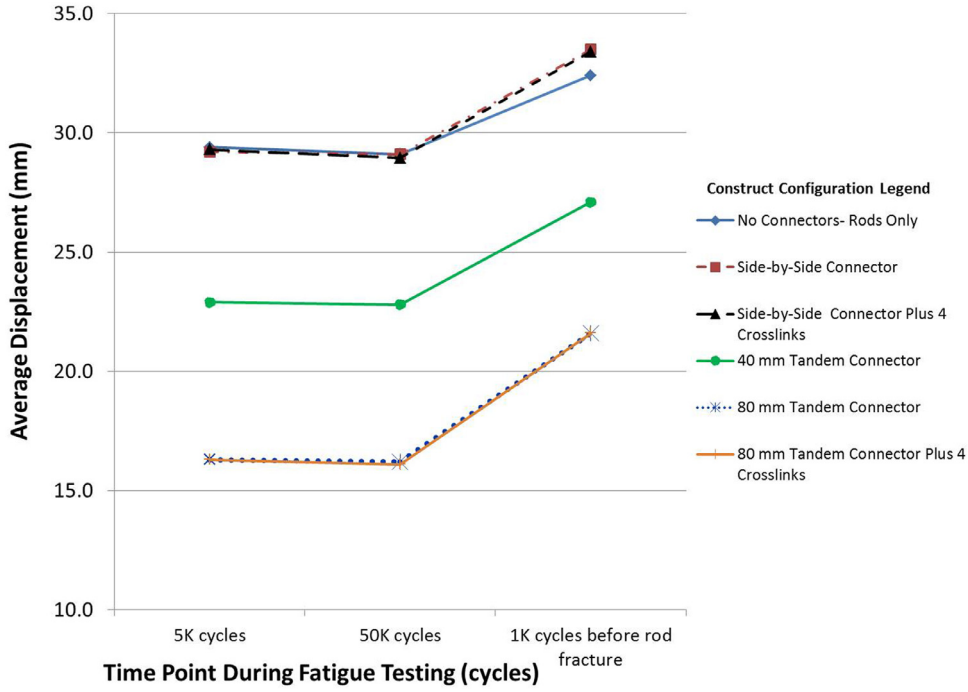

Fig. 4. Graph showing displacement over time during fatigue testing: 5000 cycles after start of the test, 50,000 cycles after start of the test, and 1000 cycles before failure. Displacement correlated to the type of axial connector, and the construct configurations with 80-mm tandem connectors (orange plus sign and blue star) allowed for the least amount of displacement. The groups with crosslinks (black triangle and orange plus sign) had similar displacements compared with their corresponding groups without crosslinks (red square and blue star, respectively). (Color version of figure is available online.).

were highly consistent with the experimentally measured values (Fig. 5). The average percent difference between the experimentally measured load and that predicted by the computational model ranged from 1.5% to 16.6% across the construct configurations and the stiffness compared favorably (Table 3). These comparisons suggest that the computational model predicts stress in the rod with a high degree of accuracy. Fig. 6 presents the maximum von Mises stresses at distinct points along the construct where components intersect (eg, rod to axial connector). The models generally predicted that stress values are high in the rod where it connects with other components. Furthermore, when subjected to compression bending, constructs with side-by-side connectors (Fig. 6B and C) exhibited the highest stress and lowest FSF overall. For constructs without crosslinks (Fig. 6A, B, D, E), the critical stress was located mid-rod for the configuration without connectors (rods only) or near the interface with the axial connector. In contrast, the model predicted a shift in the critical stress location when crosslinks were added to the construct (Fig. 6C and F) with the new critical stress

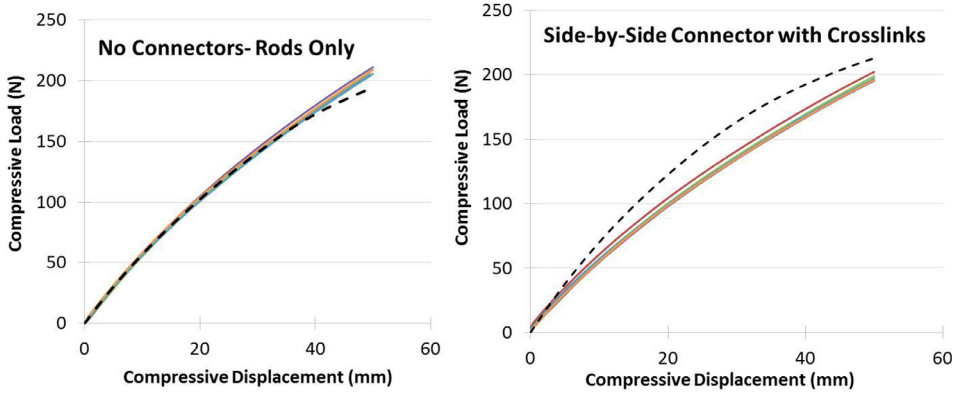

Fig. 5. Comparison of computational modeling predictions (dashed line) for construct load–displacement curve in comparison to experimental measurements (solid lines). Results are shown for the construct without connectors (rods only), which exhibited the highest level of agreement (98.5%) between the simulation and experiment as well as the side-by-side with crosslinks construct, which exhibited the lowest level of agreement (83.4%) between the simulation and experiment.

Table 3
Comparison of predicted stiffness and average force values along the length of the curve for computational models as compared with experimental data. All data are displayed as average percent difference ± standard deviation as calculated between the computational model and experimental values from six constructs. The percent difference in stiffness is calculated from experimental stiffness measurements and the stiffness predicted by the computational model over the same displacement range. The percent difference in average force is calculated from the difference in force value measured experimentally and predicted computationally at the same displacement position along the full length of the curve

	Rods only	Side-by-side connectors	40-mm Tandem connectors	80-mm Tandem connectors	
	Without crosslinks	*Without crosslinks*	*With crosslinks*	*Without crosslinks*	*Without crosslinks*	*With crosslinks*
Difference in stiffness	1.4% ± 1.8%	6.4% ± 6.9%	17.2% ± 7.7%	7.1% ± 0.1%	9.4% ± 2.8%	14.5% ± 3.1%
Difference in average force	2.1% ± 0.7%	4.7% ± 0.6%	16.3% ± 1.9%	4.5% ± 0.5%	5.4% ± 0.3%	9.0% ± 0.7%

location at the interface between the interior crosslink and rod.

Discussion

Traditional, distraction-based growing rod constructs have numerous possibilities of construct configurations because there are various types and lengths of connectors that can be chosen to achieve construct lengthening and rigidity [1]. Construct complexity is based primarily on surgeon preference and patient anatomy, but there has not been a systematic investigation of how various construct configurations may be linked to device failure. For example, it is important to understand the difference in

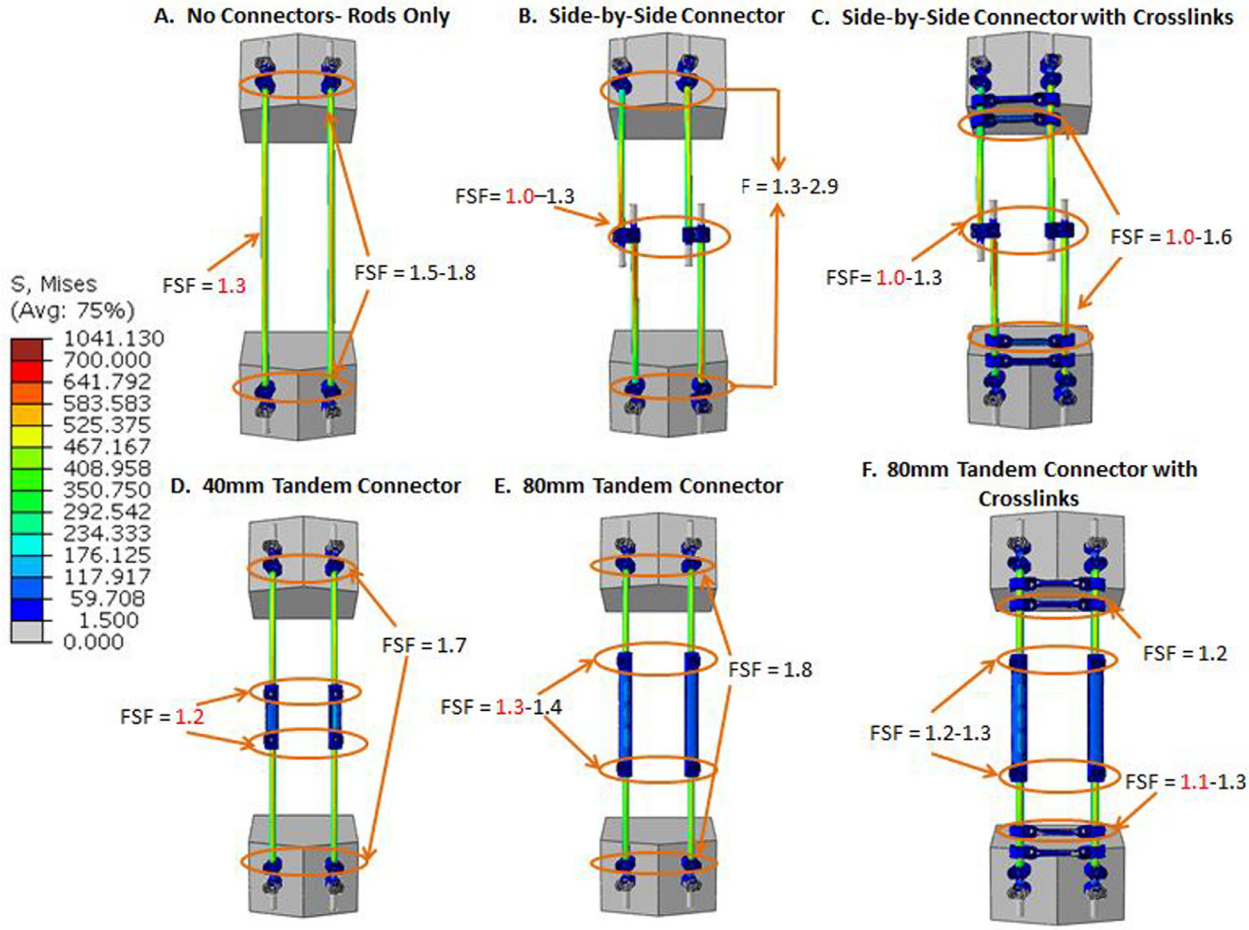

Fig. 6. Plots of Von Mises stress for each construct configuration. The fatigue safety factor (FSF) is shown within important regions of each construct where axial connectors interface with the rod and/or where they are attached to pedicle screws. The lowest FSF indicating the critical point for fatigue failure predicted by FE analysis is denoted in red font for each construct. In A, B, D, and E (constructs without crosslinks), experimental failures were observed in the rod at an interior pedicle screw. In C and F (constructs with crosslinks) experimental failure was observed in the rod adjacent to a crosslink. (Color version of figure is available online.).

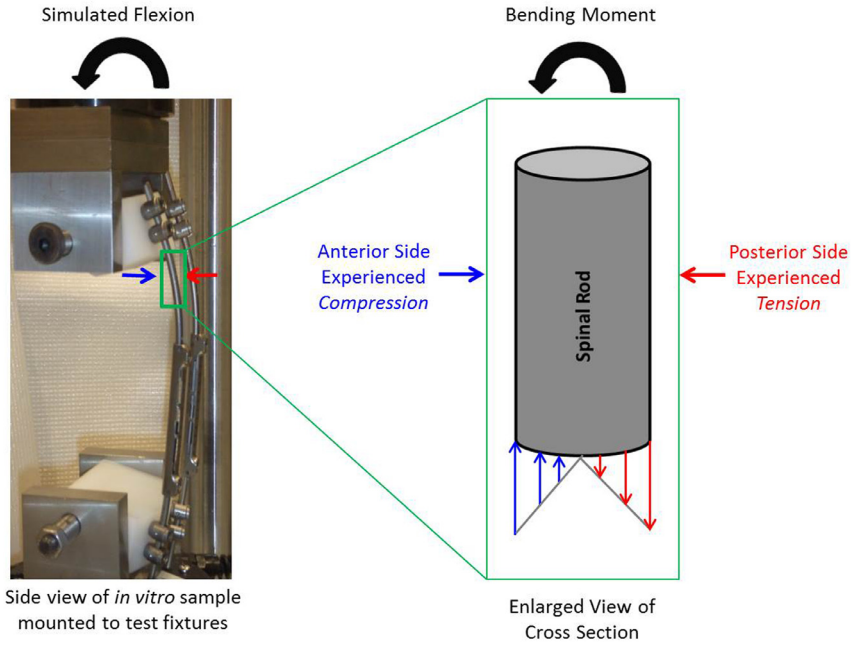

Fig. 7. Stress experienced by the posterior (red arrows) and anterior sides (blue arrows) of a spinal rod during flexion motion. Note that the spinal rods were subjected to compression bending in order to simulate spine flexion on the bench (black arrows). All rod fractures initiated on the posterior side of the rod experienced tensile stress; this is also the side of the rod where stress concentrations due to interconnecting components (eg, set screws) are located. (Color version of figure is available online.).

mechanical performance of tandem versus side-by-side connectors because the distribution of stress within the construct may change depending on the type of axial connector selected. In addition, mechanical models that can successfully simulate clinically-relevant scenarios in order to assess device performance and elucidate differences in construct configuration have not been developed. Therefore, the current study involved the development of relevant nonclinical models to predict mechanical performance of multiple types of construct configurations using traditional, distraction-based growing rods.

The mechanical bench model developed herein successfully reproduced key findings from a previous growing rod retrieval study [19]. First, the experimental bench model replicated fatigue fracture of the rod by imposing dynamic compression bending (by applying a bending moment through an offset axial load) to simulate flexion motion. Second, rod fracture for the in vitro samples initiated on the posterior side of the rod, which is the same fracture initiation site as the ex vivo samples. Mechanics of materials principles were explored to help explain this finding as depicted in Fig. 7. In this example, the spinal rod is analogous to a beam in bending. The stress of a beam in bending varies linearly from zero at the center (neutral axis) to maximum at the outer fiber of the beam. More specifically, the beam in bending causes tensile stress on one side and compressive stress on the other side, starting from the neutral axis. Therefore, during flexion of the growing rod construct, the posterior side of the rod experienced tension and the anterior side experienced compression [22]. Based on principles of fracture mechanics, crack growth typically occurs under tensile stresses that pull the tip of an existing crack open; during multiple fatigue cycles, the crack leads to final fracture. The proposed bench model allowed for the correct rod orientation so that the interconnecting components (screw or connector) interfaced with the posterior side of the rod that is experiencing tension, just as the rod would in vivo. Third, in vitro tested samples fractured adjacent to interconnecting components (eg, set screws, crosslinks) where the FE analysis predicted locally high stresses. Together, these results are consistent with a previous retrieval study that revealed 62.5% of rod fractures initiated at a stress concentration [19]. Although a mechanical bench model presents limitations when evaluating clinical performance of a device (eg, full spine was not used), the methods described herein allow for a simple, repeatable test that can recreate clinical device failures. Furthermore, the study results suggest that the mechanical bench model developed and used in this study is clinically relevant, and can serve as a useful tool for assessing the mechanical performance of growing rod construct designs.

The current study identified important differences in mechanical performance of various growing rod construct configurations using the experimental model. Based on a prior retrieval study, it was hypothesized that rigidity and lack of flexibility of the constructs were associated with rod fracture [19]. This hypothesis was supported by the current study where we found that construct rigidity (reported as stiffness) and flexibility (reported as displacement) correlated with the types and lengths of the axial connector. In other words, the construct with the longest tandem connector of 80 mm

and crosslinks was found to be the most rigid (highest stiffness from static testing) and least flexible (lowest displacement during fatigue testing). Moreover, the bench study demonstrated that crosslinks significantly decreased the fatigue performance of constructs compared with constructs without crosslinks. Crosslinks also shifted the location of fracture during dynamic testing to the local vicinity of the rod adjacent to the crosslink (Fig. 3). The more interconnecting components present in the construct may also correspond to increased probability for fracture initiation given that additional stress concentrations are created on the posterior side of the rod. Therefore, the current study confirmed that constructs with tandem connectors and multiple crosslinks decrease mechanical performance.

Computational modeling proved to be a valuable tool for predicting mechanical performance between various construct configurations. Generally, the model predicted high stresses in the rod for all construct configurations. The computational model's predictions of critical stress locations varied somewhat from fracture locations observed in experimental testing. More specifically, the computational model accurately predicted that the critical stress location coincided with the fracture location for the constructs with crosslinks, but varied from experimentally observed fracture locations for constructs without crosslinks. For example, for configurations without crosslinks, the computational model predicted that von Mises stress was highest either mid-rod or at the interface between the axial connector and rod, whereas fractures observed during experimental testing were adjacent to the pedicle screw. Generally, there was not a substantial difference in von Mises stress values between these locations predicted by the computational model and therefore, the experimentally observed fractures may have resulted not only from the high stress, but also the presence of the local deformations created by interconnecting components or microstructural features (eg, inclusion), which were not explicitly included in the computational model. Although this may be a limitation of the computational model, it did predict locally high stresses in areas where fracture was observed experimentally. Also, it was determined to be a credible method for predicting stresses in the rod based on the high degree of agreement in the load–displacement curve between the experimental and computational methods. Future work will focus on incorporating additional clinical information into the computational model to make more predictions about in vivo device performance.

This study revealed the importance of evaluating both static and dynamic test results when examining device performance. For example, static testing showed that the 80-mm tandem connector with crosslinks configuration had the highest yield load, peak load, and stiffness (Table 2). Therefore, initially it would be reasonable to assume that this construct configuration is superior in terms of mechanical performance. However, the dynamic test results demonstrated that the fatigue performance for the configuration with 80-mm tandem connectors and crosslinks is significantly lower compared with the construct configurations without crosslinks (Fig. 2). As another example, the static testing did not provide pertinent results about the flexibility of the construct, but the dynamic testing demonstrated that construct flexibility (displacement) changed throughout the test and varied based on the length of the axial connector (Fig. 4).

Several recommendations were formulated based on the results of the current research study in conjunction with the results of the prior retrieval study [19]. We recommend that surgeons consider the number of interconnecting components used in the high stress regions of a pediatric growing rod construct, that is loaded area/active length. Both the retrieval and bench studies showed that the more interconnecting components included in the construct increases the rigidity and decreases the flexibility of the system, which are correlated with earlier failure. Additionally, more interconnecting components included in the construct also increases the number of stress concentrations along the weakest side of the rod (posterior) during the primary motion of flexion. Since fracture initiated on the posterior side in all retrievals and in vitro samples, it is important to minimize the stress along that side of the rod to help reduce the rod's susceptibility to fracture. Additionally, based on our results that crosslinks were associated with earlier fatigue failure than the same construct configuration without crosslinks, we recommend that crosslinks be implanted in low stress regions of the construct (outside of the anchor foundations) rather than in the high stress regions of the construct (ie, between the anchor foundations) as observed in the prior retrieval study [19]. Shifting the location of the crosslinks would allow for an increase in torsional rigidity without affecting bending fatigue performance by reducing the stress concentration on the rod due to the interconnecting component. Serhan et al. verified that torsional stiffness could be achieved while still maintaining bending fatigue performance when the crosslinks are placed outside of the pedicle screws in the low stress region of the construct [26]. A deformed, growing spine experiences multidirectional loading while the implants keep the spine distracted to help prevent progression of a scoliotic curve and accommodate growth [1, 23–25]. Therefore, it may be more biomechanically favorable to use implants that are less rigid and allow more flexibility as opposed to rigid constructs that are inflexible with spinal motion. This concept was proposed by Yamaguchi et al.; however, bench studies were not performed to support this hypothesis [16]. The current results from both static and dynamic testing combined with those of the previous retrieval study help support this concept that rigid and less flexible constructs (ie, higher stiffness and lower displacement) demonstrate decreased mechanical performance. These recommendations along with those made in the prior retrieval study may help reduce the incidence of rod fracture and subsequent unplanned

surgeries for patients with traditional, distraction-based growing rod constructs.

Acknowledgments

We would like to thank Depuy-Synthes Spine (Raynham, MA) for donating all implants used for testing. We specifically acknowledge Hassan Serhan, PhD, Sharon Starowitz, Judi Hawker, and Andrew Dooris, PhD for their collaborative efforts and scientific input. We would also like to thank Franklin Tarke and Dikshya Parajuli for their scientific contributions.

Supplementary materials

Supplementary material associated with this article can be found, in the online version, at doi:10.1016/j.spinee.2018.09.006.

References

[1] Akbarnia BA, Yazici M, Thompson GH. The growing spine: management of spinal disorders in young children. Springer Science & Business Media; 2010.
[2] Melkerson MN, Griffith SL, Kirkpatrick JS. Spinal Implants: Are We Evaluating Them Appropriately? Astm International; 2003.
[3] Ashman RB, Birch JG, Bone LB, Corin JD, Herring JA, Charles E Johnston I, et al. Mechanical testing of spinal instrumentation. Clinical orthopaedics and related research 1988;227: 113–25.
[4] Stambough JL, Sabri EH, Huston RL, Genaidy AM, Al-khatib F, Serhan H. Effects of cross-linkage on fatigue life and failure modes of stainless steel posterior spinal constructs. Journal of Spinal Disorders & Techniques 1998;11(3):221–6.
[5] Dick JC, Zdeblick TA, Bartel BD, Kunz DN. Mechanical Evaluation of Cross-Link Designs in Rigid Pedicle Screw Systems. Spine 1997;22(4):370–5.
[6] Lynn G, Mukherjee DP, Kruse RN, Sadasivan KK, Albright JA. Mechanical stability of thoracolumbar pedicle screw fixation: the effect of crosslinks. Spine 1997;22(14):1568–72.
[7] Kuklo TR, Dmitriev AE, Cardoso MJ, Lehman Jr RA, Erickson M, Gill NW. Biomechanical contribution of transverse connectors to segmental stability following long segment instrumentation with thoracic pedicle screws. Spine 2008;33(15):E482–7.
[8] Akbarnia BA, Emans JB. Complications of growth-sparing surgery in early onset scoliosis. Spine (Phila Pa 1976) 2010;35(25):2193–204.
[9] Bess S, Akbarnia BA, Thompson GH, Sponseller PD, Shah SA, El Sebaie H, et al. Complications of growing-rod treatment for early-onset scoliosis: analysis of one hundred and forty patients. J Bone Joint Surg Am 2010;92(15):2533–43.
[10] Farooq N, Garrido E, Altaf F, Dartnell J, Shah SA, Tucker SK, et al. Minimizing complications with single submuscular growing rods: a review of technique and results on 88 patients with minimum two-year follow-up. Spine (Phila Pa 1976) 2010;35(25):2252–8.
[11] Sankar WN, Acevedo DC, Skaggs DL. Comparison of complications among growing spinal implants. Spine (Phila Pa 1976) 2010;35(23):2091–6.
[12] Zebala LP, Kuklo TR, Lenke LG, Luhmann SJ, Auerbach JD, Bridwell KH. In: Dual Growing Rod Instrumentation with Pedicle Screw Foundation at a Single Institution: Assessment of Outcomes and Complications: E-Poster# 23; 2009.
[13] Yang JS, Sponseller PD, Thompson GH, Akbarnia BA, Emans JB, Yazici M, et al. Growing rod fractures: risk factors and opportunities for prevention. Spine (Phila Pa 1976) 2011;36(20):1639–44.
[14] Wattenbarger JM, Richards BS, Herring JA. A comparison of single-rod instrumentation with double-rod instrumentation in adolescent idiopathic scoliosis. Spine 2000;25(13):1680–8.
[15] Watanabe K, Uno K, Suzuki T, Kawakami N, Tsuji T, Yanagida H, et al. Risk factors for complications associated with growing-rod surgery for early-onset scoliosis. Spine (Phila Pa 1976) 2013;38(8):E464–8.
[16] Yamaguchi KT, Skaggs DL, Mansour S, Myung KS, Yazici M, Johnston C, et al. Are rib versus spine anchors protective against breakage of growing rods? Spine Deformity 2014;2(6):489–92.
[17] Lee, C., K. S. Myung and D. L. Skaggs "Some Connectors in Distraction-based Growing Rods Fail More Than Others." *Spine Deformity* 1 (2): 148-156.
[18] Mahar AT, Bagheri R, Oka R, Kostial P, Akbarnia BA. Biomechanical comparison of different anchors (foundations) for the pediatric dual growing rod technique. Spine Journal 2008;8(6):933–9.
[19] Hill G, Nagaraja S, Akbarnia BA, Pawelek J, Sponseller P, Sturm P, et al. Retrieval and clinical analysis of distraction-based dual growing rod constructs for early onset scoliosis. The Spine Journal 2017;17(10):1506–18.
[20] International, A. (2015). ASTM F1717-15 "Standard Test Methods for Spinal Implant Constructs in a Vertebrectomy Model". West Conshohocken, PA.
[21] International, A. (2013). ASTM F136-13, Standard Specification for Wrought Titanium-6Aluminum-4Vanadium ELI (Extra Low Interstitial) Alloy for Surgical Implant Applications (UNS R56401). West Conshohocken, PA.
[22] Hibbeler RC. Mechanics of Materials. Pearson Education; 2016.
[23] Sangole AP, Aubin CE, Labelle H, Stokes IA, Lenke LG, Jackson R, et al. Three-dimensional classification of thoracic scoliotic curves. Spine (Phila Pa 1976) 2009;34(1):91–9.
[24] Stokes IA, Bigalow LC, Moreland MS. Measurement of axial rotation of vertebrae in scoliosis. Spine (Phila Pa 1976) 1986;11(3):213–8.
[25] Birchall D, Hughes D, Gregson B, Williamson B. Demonstration of vertebral and disc mechanical torsion in adolescent idiopathic scoliosis using three-dimensional MR imaging. European Spine Journal 2005;14(2):123–9.
[26] Serhan H, Giorgio P, Torres K, Slivka M. Spinal implant transverse rod connectors: A delicate balance between stability and fatigue performance. ASTM Special Technical Publication 2002;1431:34–9.